

# Internal quantum efficiency modeling of silicon photodiodes

T. R. Gentile,<sup>1,\*</sup> S. W. Brown,<sup>2</sup> K. R. Lykke,<sup>2</sup> P. S. Shaw,<sup>3</sup> and J. T. Woodward<sup>2</sup>

<sup>1</sup>Stop 8461, National Institute of Standards and Technology, Gaithersburg, Maryland 20899, USA

<sup>2</sup>Stop 8444, National Institute of Standards and Technology, Gaithersburg, Maryland 20899, USA

<sup>3</sup>Stop 8411, National Institute of Standards and Technology, Gaithersburg, Maryland 20899, USA

\*Corresponding author: thomas.gentile@nist.gov

Received 6 January 2010; accepted 15 February 2010;  
posted 25 February 2010 (Doc. ID 122268); published 30 March 2010

Results are presented for modeling of the shape of the internal quantum efficiency (IQE) versus wavelength for silicon photodiodes in the 400 nm to 900 nm wavelength range. The IQE data are based on measurements of the external quantum efficiencies of three transmission optical trap detectors using an extensive set of laser wavelengths, along with the transmittance of the traps. We find that a simplified version of a previously reported IQE model fits the data with an accuracy of better than 0.01%. These results provide an important validation of the National Institute of Standards and Technology (NIST) spectral radiant power responsivity scale disseminated through the NIST Spectral Comparator Facility, as well as those scales disseminated by other National Metrology Institutes who have employed the same model.

*OCIS codes:* 120.5630, 230.5170.

## 1. Introduction

Silicon photodiodes are widely used for accurate radiometric measurements. At the National Institute of Standards and Technology (NIST), optical trap detectors [1] consisting of three (reflectance type) or six (transmission type) silicon photodiodes, calibrated against cryogenic radiometers with laser sources, have been used to realize scales of absolute spectral responsivity in the 350 nm to 1010 nm spectral region. In 1996 a spectral radiant power responsivity scale, based on measurements of the external quantum efficiency (EQE) of three-diode (Hamamatsu S1337 [2]) reflectance trap detectors at nine laser wavelengths between 406 nm and 920 nm, combined with modeling of the internal quantum efficiency (IQE) to provide a continuous scale, was reported [3]. In that work, a model that has now become widely used and/or compared to other approaches [4–11] was developed to fit the IQE data. Currently a much more extensive set of laser wavelengths is employed to realize the same scale [12], which provides an opportunity to more carefully evaluate the significance of the form of this model. In this paper we present results for modeling the

shape of the IQE versus wavelength based on measurements of the EQE of six-diode (Hamamatsu S1337 and S6337 [2]) transmission trap detectors at 30 wavelengths between 400 nm and 900 nm. These measurements were performed on the NIST facility for Spectral Irradiance and Radiance Responsivity Calibrations using Uniform Sources (SIRCUS) [12]. We discuss the form of the model and compare its accuracy to the interpolation approach currently used to realize the spectral radiant power responsivity scale at NIST. These results provide an important validation of the NIST spectral radiant power responsivity scale disseminated through the NIST Spectral Comparator Facility [13], as well as those scales disseminated by other National Metrology Institutes who have employed the same model.

## 2. Measurements of EQE and Transmittance of Optical Trap Detectors

### A. Cryogenic Radiometer Setup in SIRCUS

Figure 1 shows the apparatus for calibration of trap detectors against an absolute cryogenic radiometer

[14] (ACR). Collimated light from either a tunable Ti:sapphire laser or tunable optical parametric oscillators (OPOs) is sent through a liquid crystal intensity stabilizer. Two spherical mirrors and a pinhole are used to spatially filter the beam. A beam splitter directs a small fraction of the light into a monitor detector used to stabilize the intensity in the light beam. A polarizer ensures the correct polarization entering the Brewster window on the ACR. Baffles between the polarizer and the ACR remove any residual scattered light from the measurement. The ACR and the trap detectors (Devices Under Test (DUT)) are on a translation stage that positions each detector in front of the incident beam sequentially. To cancel out intensity fluctuations, independent measurements of the incident laser flux with the different detectors are normalized to a monitor detector. The trap detectors are underfilled for both these measurements and the transmittance measurements discussed below.

Figure 2 shows the recent data for the external quantum efficiencies for three six-photodiode, transmission trap detectors [15] obtained using an exten-

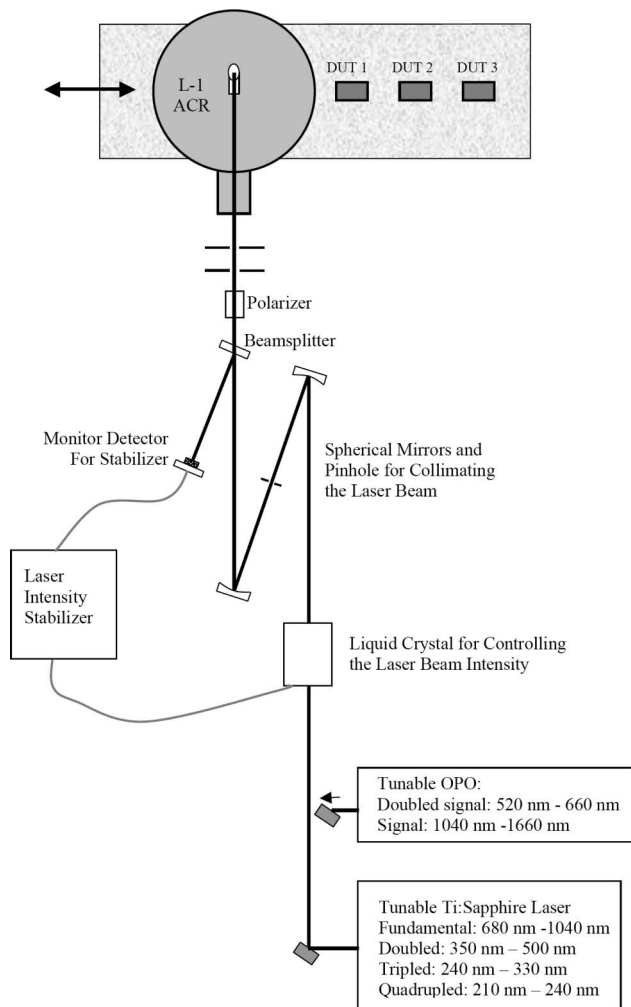


Fig. 1. Apparatus for trap calibration using the L-1 absolute cryogenic radiometer. The apparatus and measurements are discussed in the text.

sive range of laser wavelengths. To obtain a large field of view, the detectors were constructed with two Hamamatsu S1337 photodiodes [2] followed by four Hamamatsu S6337 photodiodes. Although data were obtained for the 350 nm to 1010 nm range, we only show the 400 nm to 900 nm wavelength range of interest for our IQE modeling.

## B. Transmittance Measurements

The transmittances of the optical trap detectors were measured using the experimental setup shown in Fig. 3. An optical axis was defined between a 3.8 cm (1.5 in.) diameter integrating sphere and the optical trap detector under test. An iris with an approximately 2 mm aperture was placed in front of the integrating sphere, and a 40 cm focal length lens was placed approximately halfway between the iris and the detector. The distance from the iris to the trap detector was 1.6 m. The beam stop at the back of the detector was removed, and a second optical trap detector was positioned to measure the transmitted beam. Light from the SIRCUS lasers was fiber coupled into the integrating sphere, and a monitor diode on the sphere was used as feedback for a laser power controller to stabilize the power in the sphere. The current from the optical trap detectors was measured with current to voltage amplifiers.

Figure 4 shows data for the transmittance of trap T-01 obtained at 13 wavelengths between 380 nm and 800 nm, along with the calculated transmittance for an average oxide thickness of 30.0 nm. The oxide thickness was adjusted to provide the best fit to the data between 400 nm and 800 nm, as discussed in Ref. [3]. Table 1 summarizes the values of oxide thickness we found in the literature on the reflectance of individual photodiodes, as well as the reflectance and transmittance of trap detectors. The results from this work are also listed; we obtained  $30.0 \pm 0.2$  nm for two transmission trap detectors. The results in Ref. [16], as well as the excellent

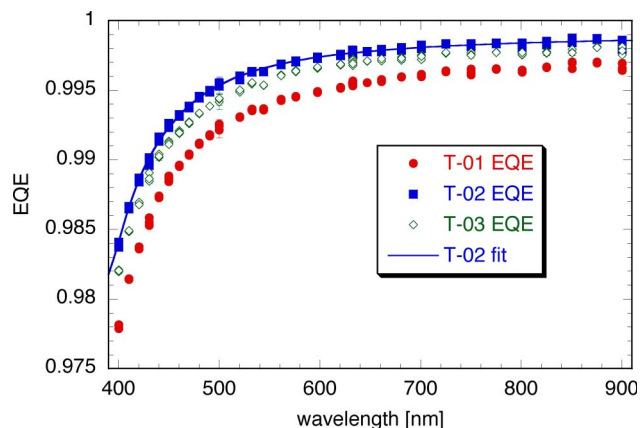


Fig. 2. (Color online) External quantum efficiency (EQE) of the transmission traps: T-01 (red solid circles), T-02 (blue solid squares), and T-03 (green open diamonds). The smooth curve shows the EQE for T-02 determined from the three-parameter IQE model [Eq. (1)] discussed in Subsection 3.B and the transmittance calculation discussed in Subsection 2.B.

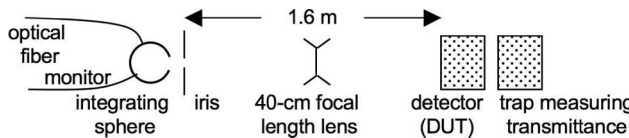


Fig. 3. Schematic of the experimental apparatus used to determine the trap transmittance. The apparatus and measurements are discussed in the text.

agreement between our data and calculation, indicate that use of an average oxide thickness for the different photodiodes in our trap (S1337 and S6337) is acceptable.

### 3. Internal Quantum Efficiency Modeling

#### A. Collection Efficiency Modeling

We begin with the IQE model that was employed for the 1996 NIST scale, which is based on the collection efficiency profile shown in Fig. 5. The most important feature of this model is a small variation of an earlier model developed by Geist *et al.* [17]. Whereas the Geist model was successful for modeling the decrease in IQE in the blue end of the spectrum, modification was required to accurately fit the data in the near-infrared. The final model assumed a linear increase in collection efficiency from a value  $P_f$  at the front of the photodiode to a value of unity at a distance  $T$  into the photodiode (following Geist), and a linear decrease in collection efficiency resulting in a value  $P_r$  at a distance  $D$  into the diode. The collection efficiency was fixed at  $P_r$  until the back of the diode, located at a distance  $h$ . This model was used to fit values of IQE determined at nine wavelengths between 406 nm and 920 nm, based on measurements of the EQE and reflectance for two three-diode (Hamamatsu 1337) reflectance traps. An extension of the model, which added a term to account for reflection of light at the back of the diode, was also introduced to extend the model to 951 nm. In this paper, our discussion is limited to the 400 nm to 900 nm range, in which including reflection from the back of the diode is not required.

#### B. Simplified Model

As presented below, we found that the IQE results in this paper can also be well fit with a simplified

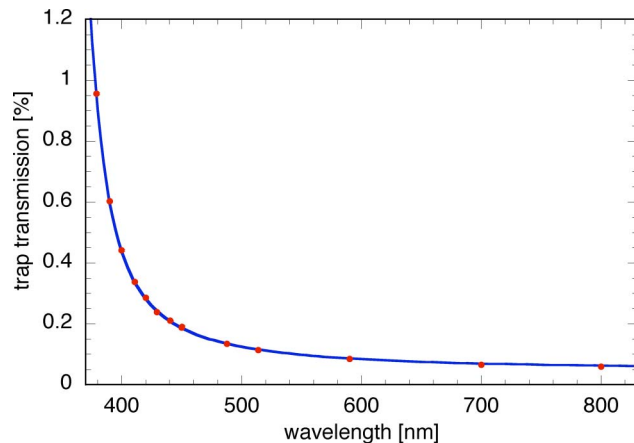


Fig. 4. (Color online) Transmittance of trap T-01. The line is the calculated transmission for an oxide thickness of 30.0 nm. The error bars are smaller than the size of the points.

version of this model (see Fig. 5). In this three-parameter model, the parameter  $D$  was eliminated; hence the collection efficiency simply rises from a value of  $P_f$  at the front of the diode to a value  $P_r$  over a distance  $T$ , and stays fixed at  $P_r$  to the back of the diode. Although again the form for the collection efficiency in the bulk of the diode is phenomenological, it is physically reasonable to assume that the collection efficiency will never be perfect.

For this model, the IQE,  $\eta_i(\lambda)$ , is given by

$$\eta_i(\lambda) = P_f + \frac{P_r - P_f}{\alpha(\lambda)T} \{1 - \exp[-\alpha(\lambda)T]\}. \quad (1)$$

As discussed in Ref. [3], the IQE values are plotted and fit with the absorption coefficient of silicon,  $\alpha(\lambda)$ , as the independent variable. The same values of the absorption coefficient as were used in Ref. [3] are also used in this paper. These values are based on a combination of the results of Jellison [18] (below 650 nm) and those of Geist *et al.* [19] (above 650 nm), as discussed in Ref. [3]. In the discussion below, we will refer to the model proposed in Ref. [3] as the “four-parameter model” and the model shown in Eq. (1) as the “three-parameter model.”

Table 1. Oxide Thicknesses Reported in the Literature as Determined from Reflectance of Individual Photodiodes, or Reflectance or Transmittance of Trap Detectors<sup>a</sup>

$O$ [nm]	$\Delta$	$\lambda$ [nm]	Measurement Information
28.84–29.53	0.2%	457–640	trap, $R$ , S1337 [4]
29.1		633	trap, $R$ , S1337 [6]
28.84–29.93	0%–3%	406–670	$R$ , single diodes [7]
28.5	0.2%	visible	$R$ , single diodes, S6337[16]
28.5	0.2%	450–650	trap, $T$ , S1337 [20]
28.05 ± 0.42	1%–3.6%	406–633	trap, $R$ , S1337 [3]
30.0 ± 0.2	0.3%	380–800	trap, $T$ , S1337 and S6337 [this work]

<sup>a</sup> $O$  is the oxide thickness,  $\Delta$  is the typical deviation between the measured and calculated reflectance or transmittance, and  $\lambda$  indicates the wavelength ranges for the determinations. In the measurement information column,  $R$  and  $T$  indicates reflectance or transmittance measurements, respectively, and the diode model numbers [2] employed are also listed.

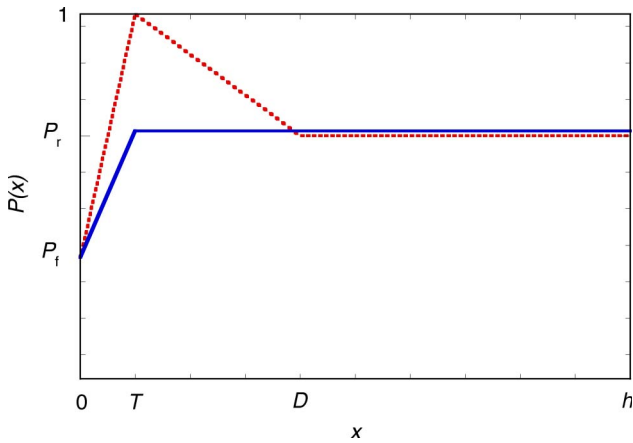


Fig. 5. (Color online) Model for the variation of the collection efficiency  $P(x)$  with distance into a photodiode of depth  $h$ . The dotted line shows the four-parameter model first employed in Ref. [3], and the solid line shows the three-parameter model employed in this paper. The parameters  $P_f$ ,  $P_r$ ,  $T$ , and  $D$  are discussed in the text.

### C. Modeling Results

The first step is to determine the IQE by correcting for the calculated transmittance  $T_t$  of the trap, where we used an oxide thickness of 30.0 nm for the calculation as discussed in Subsection 2.B. The IQE is given by the EQE divided by  $1 - T_t$ . Figure 6 shows the IQE determined from the EQE data in Fig. 2 and the calculated transmittance in Fig. 4. Figure 7 shows the residual for the fits, i.e., the difference between the data and the fits. For traps T-02 and T-03 there is little or no sign of any systematic deviation of the data from the fits. However, a systematic deviation of nearly  $\approx 0.02\%$  may be apparent for trap T-01. As T-01

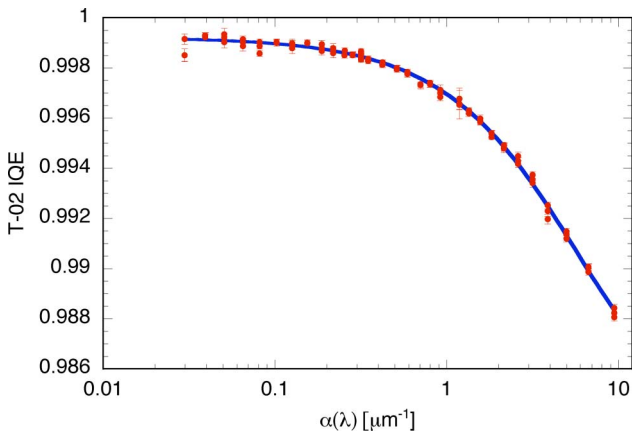


Fig. 6. (Color online) Internal quantum efficiency (IQE) for trap T-02 versus the silicon absorption coefficient  $\alpha(\lambda)$  in  $\mu\text{m}^{-1}$ , determined from the EQE measurements and the calculated transmittance for an oxide thickness of 30.0 nm. The solid line is a fit to the three-parameter model [Eq. (1)] with fitted parameters  $P_f = 0.98316 \pm 0.00026$ ,  $T = (0.31108 \pm 0.0086) \mu\text{m}$ , and  $P_r = 0.99921 \pm 0.00002$ . The error bars indicate the combined standard uncertainty, which was determined by adding the standard deviation of the trap and cryogenic radiometer signals, and an estimate of 0.01% for Type B uncertainties [21], in quadrature. The reduced  $\chi^2$  for the fit is 98/100. For clarity, the estimated uncertainties of 20% in the absorption coefficient [3] are not shown.

has the lowest EQE values, this suggests that there could be some correlation between decreased trap performance and fit quality, perhaps because one or more diodes in the trap have larger internal losses for some reason. We have not found that the parameter  $D$  improves the fits, and thus we conclude that it may have no physical significance. The behavior of the IQE in the near-infrared seems to be well described by the single parameter  $P_r$ .

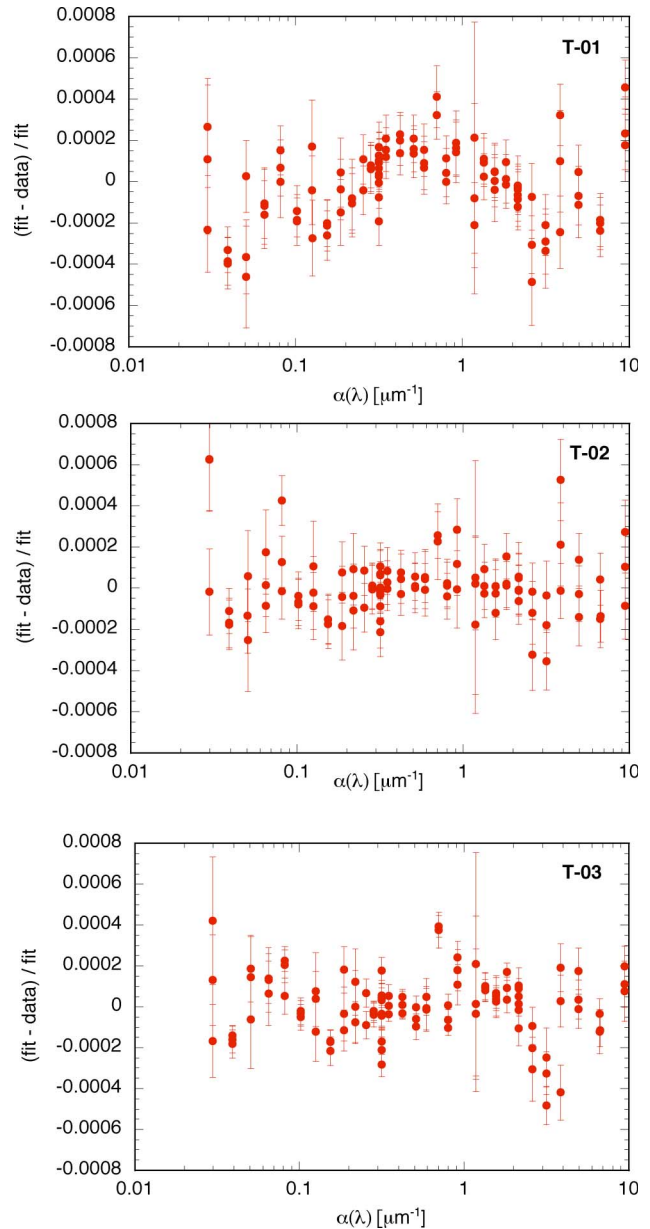


Fig. 7. (Color online) Residuals (fractional difference between fit and data for IQE) for the three traps (top to bottom, T-01 to T-03). The fitted parameters for T-02 are listed in the caption for Fig. 6; the parameters for trap T-01 are  $P_f = 0.97661 \pm 0.00022$ ,  $T = (0.35102 \pm 0.0065) \mu\text{m}$ , and  $P_r = 0.99736 \pm 0.00002$  (reduced  $\chi^2 = 178/100$ ), and for trap T-03 are  $0.98102 \pm 0.00024$ ,  $T = (0.3258 \pm 0.0076) \mu\text{m}$ , and  $P_r = 0.99861 \pm 0.00002$  (reduced  $\chi^2 = 119/100$ ).

In the 1996 scale it was found that the parameter  $D$  was not well determined [3]; this same observation was also noted more recently, but for a smaller wavelength range (400 nm–700 nm) [7]. Unfortunately a more extensive series of measurements on the traps used for the 1996 scale is not available, hence we cannot say whether the parameter  $D$  simply arose out of experimental uncertainties or was truly a feature of those traps. The question arises as to whether there was sufficient justification for introducing  $D$  based on the more limited data set in Ref. [3]. Taking another look at fitting that data, we find that the reduced  $\chi^2$  for the three-parameter model is 1.9, whereas it is 0.06 for the four-parameter model ( $D = 29 \mu\text{m} \pm 19 \mu\text{m}$ ). Whereas this large difference was certainly a good motivation for introducing  $D$  to provide a good interpolation of the data, the extremely low reduced  $\chi^2$  is a warning sign of overfitting. We also note that the effect of reflection from the back of the photodiode was estimated to be 0.06% in Ref. [3] for the point at 920 nm; hence not including this effect in the fit may have increased the value of the parameter  $D$ . (Indeed, when the reflection was taken into account in that work, the parameter  $D$  was reduced to  $D = 16 \mu\text{m} \pm 14 \mu\text{m}$ ). If this last point is removed, the reduced  $\chi^2$  for the three-parameter model decreases to a value of 0.7, which is quite reasonable. (However, the value of  $T$  drops to  $0.20 \mu\text{m}$ , which is far from the values noted in Fig. 7 and from typical values reported elsewhere.) Overall, the changes in the scale for these different fitting options are still within the uncertainties quoted in Ref. [3], thus verifying the stated accuracy of this earlier NIST scale realization. Based on these considerations, we believe that eliminating the parameter  $D$  is not inconsistent with the data in Ref. [3] that originally led to its introduction. Finally, we should consider what has been observed by other researchers, but unfortunately, full information is not always available in published literature. In Ref. [4] a fitted value of  $D = 31 \mu\text{m}$  was reported, but the uncertainty was not reported and their data did not extend into the red beyond 650 nm. In Ref. [6] a fitted value

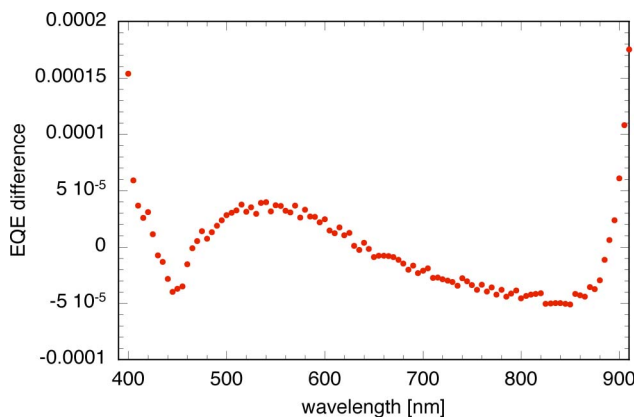


Fig. 8. (Color online) Difference between the EQE for trap T-02 determined from the IQE fit and from interpolation using Eq. (2).

of  $D = 16 \mu\text{m}$  was reported, but the uncertainty was also not reported. In Ref. [7], a value of  $D = (3.0 \pm 3.2) \mu\text{m}$  was reported; their data set did not extend beyond 700 nm. In Ref. [10] the model was employed, but no parameters were reported. Hence it is difficult for us to evaluate whether other researchers have found that  $D$  is truly a meaningful parameter.

At present we conclude that the three-parameter model fits the extensive data for three transmission traps with high accuracy. Figure 2 shows the modeled EQE for trap T-02, determined from the three-parameter IQE model and the transmittance calculation. The modeled EQE was determined from the product of the modelled IQE and  $1 - T_t$ .

#### D. Model Accuracy

Presently the scale at NIST is realized by fitting the data for EQE versus wavelength  $\lambda$ , for the full range between 350 nm and 1010 nm, to a phenomenological nine-parameter functional form consisting of two Lorentzian functions ( $b$  and  $c$  fit parameters) plus an exponentially decaying function ( $a$  fit parameters):

$$\text{EQE}(\lambda) = \frac{a_1}{1 + \exp[-(\lambda - a_2)/a_3]} - \frac{b_1}{1 + (\lambda - b_2)^2/b_3^2} - \frac{c_1}{1 + (\lambda - c_2)^2/c_3^2}. \quad (2)$$

Figure 8 shows a comparison of this interpolation for trap T-02 and the EQE determined from the three-parameter IQE model. The approaches agree within 0.005% over almost all of the 400 nm to 900 nm range. There is a steep increase in the difference between the two approaches at the 400 nm and 900 nm endpoints. The differences are similar for trap T-03, but are roughly doubled to 0.01% for trap T-01.

Figure 9 shows the variation in the IQE model for variations of the fitted parameters by their uncertainties. Results are shown for an increase in each

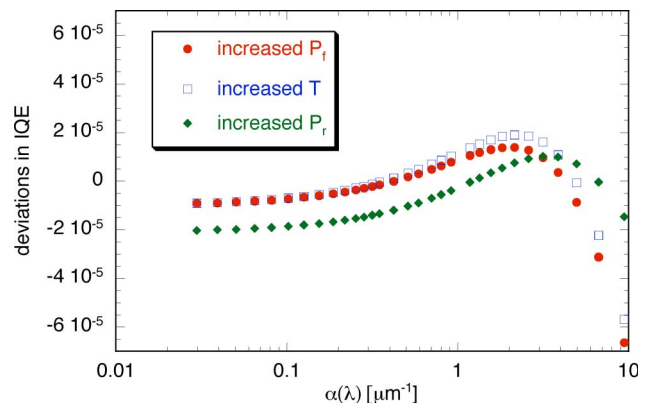


Fig. 9. (Color online) Deviations of the fitted values for the IQE of trap T-02 for an increase of a given fitted parameter by its uncertainty, while refitting all other parameters. Key for shifts: increased  $P_f$  (red, solid circles), increased  $T$  (blue, open squares), and increased  $P_r$  (green, solid diamonds).

parameter's value; a decrease yields a symmetric deviation about zero. The variations are typically 0.002%, increasing to 0.006% at the blue end of the spectrum. Based on the results shown in Figs. 8 and 9, we conclude that the relative standard uncertainty in the EQE determined from the IQE model and the transmittance is typically about 0.005%.

From a practical point of view, it is of interest to estimate how accurately IQE data can be fit for a much more limited range of data. Experimenting with decreasing the number of wavelengths in the current data set for trap T-02 from 33 down to 7 or 9 reveals that the uncertainties in the fit parameters varies roughly as the square root of the number of degrees of freedom. (For this test we used one data point for each laser wavelength; hence the number of degrees of freedom is the number of wavelengths minus three.) Hence a scale with a relative standard uncertainty of  $\approx 0.01\%$  should be possible with many fewer wavelengths, for the typical measurement uncertainties of 0.01% to 0.02% in the current data set. Based on Fig. 9, measurements should be concentrated at the blue end of the spectrum, which is not a surprising result.

#### 4. Conclusions

We have employed the IQE model from Ref. [3] to an extensive series of accurate EQE measurements on three transmission traps and found that a simplified, three-parameter variation of this model allows for accurate fitting of these data for the 400 nm to 900 nm wavelength range. The results indicate that the model can be used to interpolate between a fairly small number of measurements with accuracy comparable to the accuracy of each measurement. The results have also empirically validated the historical spectral radiant power responsivity scale disseminated by NIST at the estimated uncertainty.

T. R. Gentile thanks G. P. Eppeldauer (NIST) for motivating this work.

#### References and Notes

1. E. F. Zalewski and C. R. Duda, "Silicon photodiode device with 100% external quantum efficiency," *Appl. Opt.* **22**, 2867–2873 (1983).
2. Hamamatsu Corporation, 360 Foothill Road, Bridgewater, New Jersey 08807, USA.
3. T. R. Gentile, J. M. Houston, and C. L. Cromer, "Realization of a scale of absolute spectral response using the National Institute of Standards and Technology high-accuracy cryogenic radiometer," *Appl. Opt.* **35**, 4392–4402 (1996).
4. F. Sametoglu, "Establishment of illuminance scale at UME with and accurately calibrated radiometer," *Opt. Rev.* **13**, 326–337 (2006).
5. A. Ferrero, J. Campos, A. Pons, and A. Corrons, "New model for the internal quantum efficiency of photodiodes based on photocurrent analysis," *Appl. Opt.* **44**, 4392–4403 (2005).
6. J. Gran and A. S. Sudbo, "Absolute calibration of silicon photodiodes by purely relative measurements," *Metrologia* **41**, 204–212 (2004).
7. J. Campos, A. Pons, and P. Corredera, "Spectral responsivity scale in the visible range based on single silicon photodiodes," *Metrologia* **40**, S181–S184 (2003).
8. C. Hicks, M. Kalatsky, R. A. Metzler, and A. O. Goushcha, "Quantum efficiency of silicon photodiodes in the near-infrared spectral range," *Appl. Opt.* **42**, 4415–4422 (2003).
9. J. Hartmann, J. Fischer, U. Johannsen, and L. Werner, "Analytical model for the temperature dependence of the spectral responsivity of silicon," *J. Opt. Soc. Am. B* **18**, 942–947 (2001).
10. L. Werner, J. Fischer, U. Johannsen, and J. Hartmann, "Accurate determination of the spectral responsivity of silicon trap detectors between 238 nm and 1015 nm using a laser-based cryogenic radiometer," *Metrologia* **37**, 279–284 (2000).
11. T. Kùbarsepp, P. Kàrhà, and E. Ikonen, "Interpolation of the spectral responsivity of silicon photodetectors in the near ultraviolet," *Appl. Opt.* **39**, 9–15 (2000).
12. S.W. Brown, G. P. Eppeldauer, and K. R. Lykke, "Facility for spectral irradiance and radiance responsivity calibrations using uniform sources," *Appl. Opt.* **45**, 8218–8236 (2006).
13. T. C. Larason, S. S. Bruce, and A. C. Parr, *Spectroradiometric Detector Measurements* (U. S. Government Printing Office, 1998).
14. L-1 Standards and Technology, New Windsor, Maryland, USA. Certain trade names and company products are mentioned in the text or identified in an illustration in order to adequately specify the experimental procedure and equipment used. In no case does such identification imply recommendation or endorsement by the National Institute of Standards and Technology, nor does it imply that the products are necessarily the best available for the purpose.
15. G.P. Eppeldauer and D. C. Lynch, "Opto-mechanical and electronic design of a tunnel-trap Si radiometer," *J. Res. Natl. Inst. Stand. Technol.* **105**, 813–828 (2000).
16. A. Haapalinna, P. Kàrhà, and E. Ikonen, "Spectral reflectance of silicon photodiodes," *Appl. Optics* **37**, 729–732 (1998).
17. J. Geist, E. F. Zalewski, and A. R. Schaefer, "Spectral response self-calibration and interpolation of silicon photodiodes," *Appl. Opt.* **19**, 3795–3799 (1980).
18. G. E. Jellison, Jr., "Optical functions of silicon determined by two-channel polarization modulation ellipsometry," *Opt. Mater.* **1**, 41–47 (1992).
19. J. Geist, A. Migdall, and H. P. Baltes, "Analytic representation of the silicon absorption coefficient in the indirect transition region," *Appl. Opt.* **27**, 3777–3779 (1988).
20. T. Kùbarsepp, P. Kàrhà, and E. Ikonen, "Characterization of a polarization-independent transmission trap detector," *Appl. Opt.* **36**, 2807–2812 (1997).
21. B. N. Taylor and C. E. Kuyatt, "Guidelines for evaluating and expressing the uncertainty of NIST measurement results," NIST Tech. Note 1297 (National Institute of Standards and Technology, 1994). This reference is available on line at <http://physics.nist.gov/Pubs/guidelines/TN1297/tn1297s.pdf>.